

Antiferromagnetism and superconductivity: Cuprate plane magnetic ordering in $\text{YSr}_2\text{Cu}_{2.1}\text{Nb}_{0.9}\text{O}_{8-\delta}$

H. A. Blackstead,¹ W. B. Yelon,² M. Kornecki,¹ M. P. Smylie,¹ Q. Cai,³ J. Lamsal,³ V. P. S. Awana,^{4,5} S. Balamurugan,⁶ and E. Takayama-Muromachi⁶

¹*Department of Physics, University of Notre Dame, Notre Dame, Indiana 46556, USA*

²*Materials Research Center and Department of Chemistry, University of Missouri-Rolla, Rolla, Missouri 65409, USA*

³*Department of Physics, University of Missouri-Columbia, Columbia, Missouri 65211, USA*

⁴*National Physical Lab, New Delhi-110012, India*

⁵*ICYS Centre, National Institute for Material Science, Tsukuba, Ibaraki, 305-0044, Japan*

⁶*National Institute for Materials Science, Tsukuba, Ibaraki, 305-0044, Japan*

(Received 25 January 2007; published 27 April 2007)

$\text{YSr}_2\text{Cu}_{2.1}\text{Nb}_{0.9}\text{O}_{8-\delta}$, prepared using a high-pressure, high-temperature process, has been studied using superconducting quantum interference device magnetometry, neutron diffraction, and electron spin resonance (ESR). This material, in which Cu is the only magnetic ion, shows two magnetic transitions below room temperature, at 257 and 27 K. While neutron diffraction fails to find antiferromagnetic Bragg peaks, ESR unambiguously shows that the compound is antiferromagnetic. Antiferromagnetic resonance is observed for temperatures below to slightly above the lower ordering temperature. The magnetization data can be understood as arising from ferromagnetic CuO_2 planes, which are coupled as (independent) antiferromagnetic bilayers at the upper transition and then subsequently show full, three-dimensional order at the lower transition. This lightly hole-doped material shows a small diamagnetic response, closely coincident with the lower magnetic transition. The difference in field-cooled and zero-field-cooled magnetization curves is attributed to metamagnetism, arising from the weak coupling of the cuprate plane bilayers. The field-cooled magnetization data are strikingly similar to that reported for the so-called “ferromagnetic” superconductor $\text{GdSr}_2\text{Cu}_2\text{RuO}_8$, for which the anomalous magnetization has been attributed to Ru moment canting. The absence of any magnetic ion other than Cu in this compound excludes that explanation.

DOI: [10.1103/PhysRevB.75.140514](https://doi.org/10.1103/PhysRevB.75.140514)

PACS number(s): 74.72.Bk, 75.50.Ee

INTRODUCTION

The charge-balanced insulating host material $\text{YSr}_2\text{Cu}_2\text{NbO}_8$ (see Fig. 1) is a homolog of the magnetic superconductor¹ $\text{GdSr}_2\text{Cu}_2\text{RuO}_8$ which exhibits magnetism associated with ordering of the RuO_2 sublattice. This is widely believed to be due to ferromagnetism or canting of the Ru moments, although neutron diffraction finds conventional antiferromagnetism and no evidence for canting.^{2,3} Due to the very large neutron absorption cross section of natural Gd, it is necessary to use only selected Gd isotopes in samples in order to study the magnetism by neutron diffraction. Alternatively, the replacement of Gd with Y would enable neutron studies,⁴ but unfortunately, this material does not readily form at atmospheric pressure.

In order to isolate a possible Cu contribution to the magnetism and enable neutron diffraction, we replaced the magnetic Gd in $\text{GdSr}_2\text{Cu}_2\text{RuO}_8$ with Y and the magnetic Ru with nonmagnetic Nb. The material was prepared using a high-pressure, high-temperature (HPHT) process. By substituting 10% lower valence Cu for Nb^{5+} in the NbO_2 layer, light hole doping was used to facilitate the formation of single phase material. The constituents, per mole of product ($0.45\text{Nb}_2\text{O}_5$, 0.5SrO_2 , 1.5SrCuO_2 , 0.6Cu metal powder and $0.5\text{Y}_2\text{O}_3$) were thoroughly ground together using an agate mortar and pestle in a glove box under Ar. Approximately 500 mg of the raw mixture was loaded and sealed into a gold capsule. Samples of this material were then processed at 6 GPa and 1450 °C for 2 h in a flat-belt system, and allowed

to cool rapidly. The pressure was slowly released. To test for possible oxygen loss, the pellets were carefully weighed before and after processing. No significant weight change was found, indicating that the oxygen content was preserved. No post-processing annealing was performed.

NEUTRON DIFFRACTION STUDIES

Neutron diffraction was carried out at the University of Missouri Research Reactor (MURR) using a position sensitive detector system with a neutron wavelength of 1.4875 Å at a temperature of 16 K. This instrument collects a 20° section of the diffraction pattern at each setting; the full diagram is measured in five steps. Because of the unusual neutron optics and the large area detector, the throughput of the instrument is high, an essential element in following the temperature dependence of the magnetic scattering and especially in collecting data of sufficient statistical accuracy to allow refinement of the low temperature magnetic structure. Refinement of the neutron diffraction data was carried out using the FULLPROF suite of programs.⁵ The neutron measurements used about 1 g of sample, contained in a 3 mm diameter V cell. The results are given in Fig. 2. The residual of the Rietveld fit is small, and there are no indications of any contaminant phases at roughly the 1% level. Examination of the full data at the lowest temperature showed no evidence for an enlarged unit cell, i.e., no additional Bragg peaks with 1/2 integer indices were observed. In addition, partial data sets covering the low angle region were collected

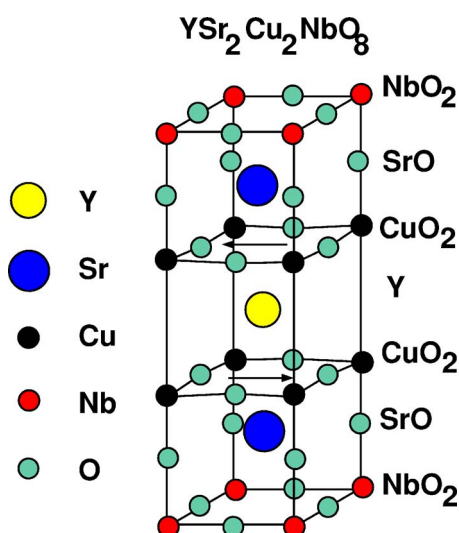


FIG. 1. (Color online) Structure of $\text{YSr}_2\text{Cu}_2\text{NbO}_8$. This structure is closely similar to that of $\text{YBa}_2\text{Cu}_3\text{O}_7$ in which Nb has replaced the chain-layer Cu, and Sr has replaced Ba. The arrows indicate the proposed magnetic structure. The magnetizations of the ferromagnetic CuO_2 layers are stacked antiferromagnetically.

with 10 times greater counting time than utilized for the full data set and subtraction of higher temperature (up to 150 K) data from the lowest temperature data revealed no additional scattering. On this basis we can exclude magnetic structures in which the unit cell is doubled in the basal plane direction(s), at a level of $\sim 0.1\mu_B$.

MAGNETIZATION

The magnetization, measured in the three configurations, zero-field-cooled (ZFC), field-cooled, and field-cooled-

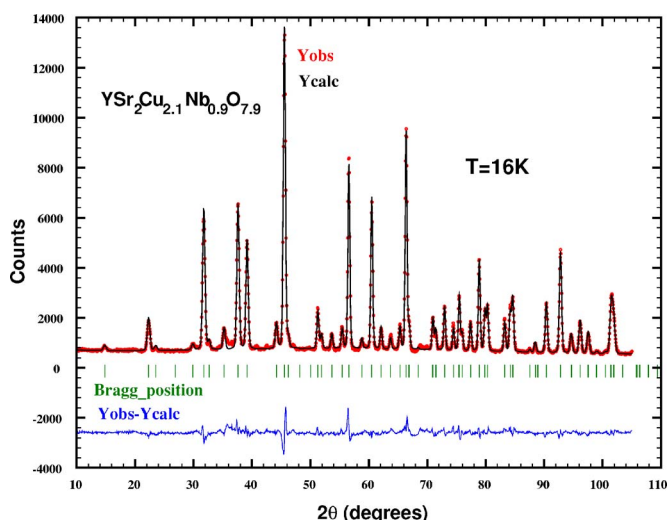


FIG. 2. (Color online) Neutron diffraction data (red points) and Rietveld fit (solid black line) obtained at 16 K. The residual at the bottom (blue) is quite small with no indication of impurity phases at the $\sim 1\%$ level. The “tic” marks show the positions of the nuclear Bragg reflections. These data, taken over a 2θ range of 10° – 100° show no magnetic peaks, indicating that the Cu order is not simple antiferromagnetism.

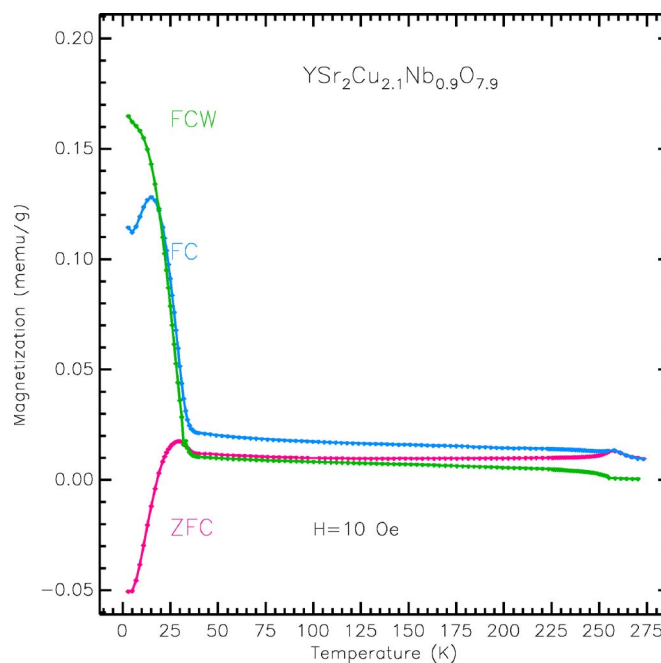


FIG. 3. (Color online) Magnetization as a function of temperature in three configurations ZFC, FC, and FCW. The data indicate an antiferromagnetic transition at $T_N=257$ K, followed at $T_c=27$ K by superconductivity, and a coincident magnetic transition which is attributed to three-dimensional antiferromagnetic ordering of the CuO_2 planes.

warming (FCW) are shown in Fig. 3. Three transitions are indicated: The ZFC data show an antiferromagnetic transition at ~ 257 K = T_N , followed at ~ 27 K = T_c by a second antiferromagnetic transition, with a nearly coincident superconducting transition as indicated by the appearance of diamagnetism. The FC data suggest a ferromagnetic-like response with superimposed diamagnetism for temperatures less than T_c , while the FCW data show that flux is effectively trapped in the superconducting state. Small flux trapping persists to nearly T_N . Field-dependent magnetization data are presented in Fig. 4. These data suggest the presence of a paramagnetic moment whose response is the dominant feature at the lowest temperatures. The black line in the figure is the magnetization resulting from $\sim 0.65\mu_B$ and a 10% content computed using the Brillouin function. This suggests that the “chain-site” dopant Cu are not ordered, at least to 3 K. The temperature-dependent magnetization data are similar in shape to that of $\text{GdSr}_2\text{Cu}_2\text{RuO}_8$, shifted to lower temperatures. In the present case, since the material contains no Ru, it is certain that the so-called “ferromagnetic” response seen in the FC and FCW data is due to ordered Cu.

MAGNETIC RESONANCE

The magnetic resonance spectrometer employed for these measurements, incorporates a TE_{101} resonant cavity⁶ with the sample mounted in the center of the cavity bottom. The rf magnetic field (H_{rf}) in the center of the bottom is uniform in direction, and the static field which was varied to a maximum of 1.9 T was applied in the plane of the cavity bottom,

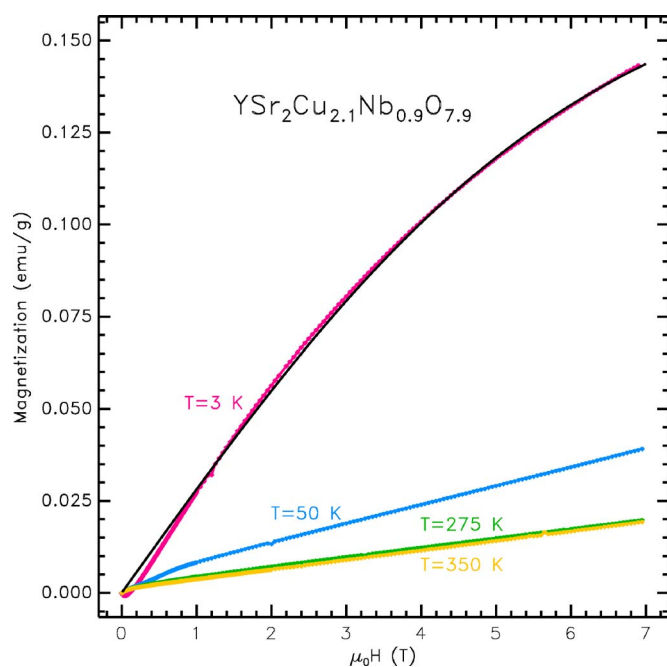


FIG. 4. (Color online) Magnetization as a function of applied field for temperatures of 3, 50, 275, and 350 K. The black line is computed using the Brillouin function and a magnetic moment of $0.65\mu_B$. These data suggest that the “chain-site” dopant Cu are not ordered. In addition, the data at higher temperatures show a paramagnetic linear response with a superimposed low field saturation.

and could be rotated in that plane to be either parallel or perpendicular to H_{rf} . With this capability, the resonance data were obtained with two rf-dc field configurations, see Figs. 5 and 6. If the system were paramagnetic, ferromagnetic, or ferrimagnetic, resonance could only be excited with $H_{dc} \perp H_{rf}$, while for antiferromagnetic or weakly ferromagnetic spin configurations the selection rules are such that

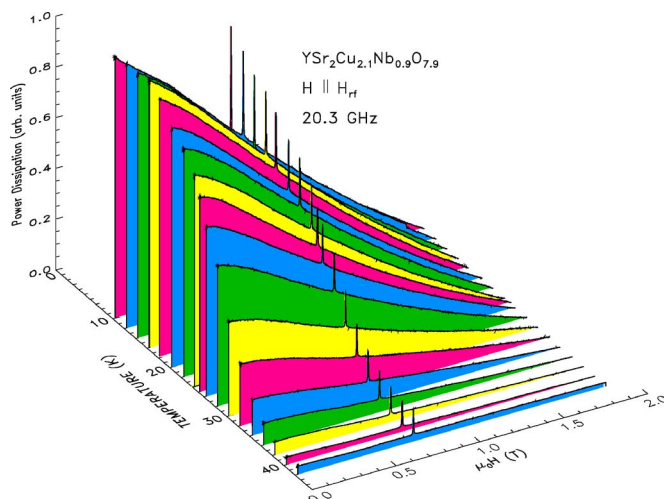


FIG. 5. (Color online) Antiferromagnetic resonance data as functions of applied field and temperature with two rf-dc field configurations. In the left panel, data with $H \parallel H_{rf}$ are given. In this configuration, the rf torque vanishes for paramagnets and ferromagnets, and no resonance is possible. The selection rules permit antiferromagnetic resonance for this configuration.

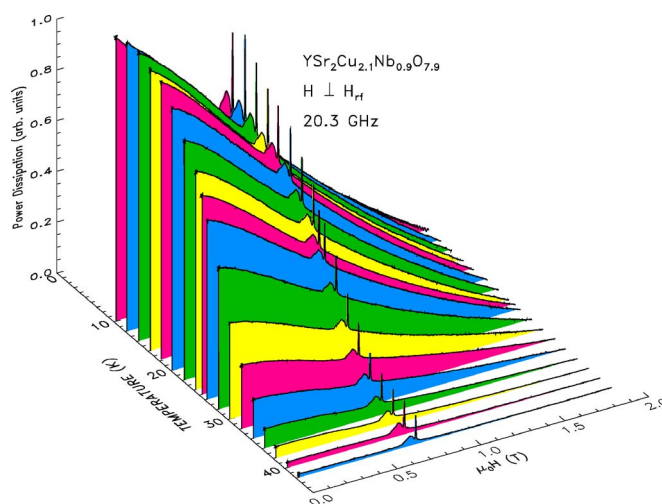


FIG. 6. (Color online) In the right panel, $H \perp H_{rf}$. In this case, a small ESR response is indicated near the sidewall mounted $g=2$ paramagnetic marker. This is likely the “chain-site” Cu which is seen in the magnetization data, or else a small content of impurity SrCuO_2 . These data demonstrate that the cuprate plane Cu are antiferromagnetically ordered.

resonance can be excited⁷ both with $H_{dc} \perp H_{rf}$ and with $H_{dc} \parallel H_{rf}$. Thus, the data of Fig. 5, combined with the magnetization data which are linear in H , demonstrate that the Cu spins are ordered in an antiferromagnetic configuration. The energy gap for the Cu spins exceeds the microwave photon energy; as a result only the high-field part of the broad response is seen. The breadth of the response indicates a very short spin-spin relaxation time, $\sim 10^{-12}$ s. Similar cuprate plane resonances have also been found in $\text{PrBa}_2\text{Cu}_4\text{O}_8$; in this case, the cuprate planes are believed to be insulating.⁸

A sample of the free-radical bearing compound dpph was mounted on the cavity sidewall, in a position such that the rf field was always perpendicular to the applied field. As a result, the dpph response was used to compare the data from both configurations. In addition to the dpph signal, a paramagnetic spin with a g factor slightly larger than 2 is detected superimposed on the broad response. This could be due to the chain layer dopant or else to an undetected content of an impurity, which most likely would be SrCuO_x .

DISCUSSION

The magnetization, neutron diffraction data, and ESR results place constraints on the character of the magnetic order which is exhibited by the cuprate planes. Since no magnetic peaks were found in the neutron diffraction which would arise from simple antiferromagnetic spin configurations, e.g., three-dimensional antiferromagnetism with adjacent spins oppositely aligned, a configuration which does not lead to unit cell doubling is suggested, see Fig. 1. The data are consistent with a structure in which the cuprate planes order ferromagnetically, but nearest-neighbor pairs of planes (across the Y planes) are stacked antiferromagnetically. At the Néel temperature $T_N=257$ K, pairs of planes are thought to be so ordered without long range coherence; the coupling

between adjacent pairs of planes is likely so weak that the stacking of pairs of planes is largely uncorrelated. Near T_c , correlation of pairs of planes increases and full three-dimensional ordering occurs. As this temperature is approached from above, the antiferromagnetic magnetic resonance signal intensity at 20.3 GHz gradually rises, presumably coincident with the appearance of short-range order of adjacent pairs of planes. Perhaps surprisingly, this is also the onset temperature for superconductivity. The long-range, antiferromagnetic stacking of ferromagnetic CuO_2 planes will lead to an enhanced intensity of the (0,0,1) nuclear reflection. Unfortunately, the angular scan did not go to a sufficiently small 2θ to detect this signal, but previous⁴ and recent⁹ work on $\text{YSr}_2\text{RuCu}_2\text{O}_8$ has shown the enhancement of the (0,0,1) reflection in that homologous material.

The large magnetic response seen in the FC configuration for $T < T_c$ is the metamagnetic response resulting from the rotation of planes relative to each other. In the temperature interval $T_c < T < T_N$, the pairs of planes are “locked” antiferromagnetically due to the dominance of short range exchange interactions. As the temperature is lowered, the super-exchange path Cu-O-Nb-O-Cu across the SrO-NbO-SrO layers competes with the path Cu-O-Y-O-Cu through the CuO_2 -Y- CuO_2 layers, driving the transition at T_c to three-dimensional antiferromagnetic order. With this competition, application of even a small magnetic field induces rotation of the planes relative to each other, leading to a relatively large magnetization⁹ seen in the FC data of Fig. 3. No evidence for field induced ferromagnetism is seen in the high field magnetization results.

Near T_N , the antiferromagnetic spin energy gap for pairs of planes is too large for strong excitation at the frequency

utilized in this study, however, with the competition of the two super-exchange paths, the gap is lowered sufficiently and broad antiferromagnetic resonances are readily observed even for $T > T_c$.

$\text{GdSr}_2\text{Cu}_2\text{RuO}_8$ differs from the material studied here only by the substitution of magnetic Ru for nonmagnetic Nb, and nonmagnetic Y for Gd. The addition of superexchange from the Ru ion, or enhancement of the superexchange by the nonclosed Ru shell, likely raises the temperature at which three-dimensional order occurs in the CuO_2 planes. If this is the case, similar magnetic resonance should be observable from the CuO_2 planes at temperatures well above the Ru ordering temperature,¹⁰ as indeed we have observed.¹¹ In addition, ferromagnetic-like magnetization will be observed in FC measurements, and this magnetization will not arise from the RuO_2 layer, although its antiferromagnetic ordering will be indirectly responsible for the enhanced Cu ordering.

In conclusion, we have identified antiferromagnetic resonance arising from magnetically ordered cuprate planes. In addition, we have suggested a magnetic ordering model which is consistent with our neutron diffraction and resonance data, consisting of ferromagnetic cuprate planes coupled antiferromagnetically. The simple antiferromagnetic structures observed in underdoped $\text{YBa}_2\text{Cu}_3\text{O}_{7-\delta}$ are not found.

ACKNOWLEDGMENTS

V.P.S.A. thanks the ICYS Centre, NIMS, Japan for his current visit to Japan to work on HPHT synthesis of novel oxides. He further acknowledges the keen interest of Director NPL, India in the present work.

¹L. Bauernfeind, W. Widder, and H. F. Braun, *Physica C* **254**, 151 (1995).

²O. Chmaissem, J. D. Jorgensen, H. Shaked, P. Dollar, and J. L. Tallon, *Phys. Rev. B* **61**, 6401 (2000).

³J. W. Lynn, B. Keimer, C. Ulrich, C. Bernhard, and J. L. Tallon, *Phys. Rev. B* **61**, R14964 (2000).

⁴H. Takagiwa, J. Akimitsu, H. Kawano-Furukawa, and H. Yoshizawa, *J. Phys. Soc. Jpn.* **70**, 333 (2001).

⁵J. Rodriguez-Carvajal, FULLPROF.2K (version 3.00), Laboratory Leon Brillouin-JRC, 2004.

⁶C. P. Poole, Jr., *Electron Spin Resonance* (Interscience Publishers, New York, 1967), p. 264.

⁷E. A. Turov, *Physical Properties of Magnetically Ordered Crystals* (Academic Press, New York, 1965), p. 157.

⁸H. A. Blackstead, J. D. Dow, M. Osada, and M. Kakihana (unpublished).

⁹W. B. Yelon, Q. Cai, Jagat Lamsal, H. A. Blackstead, M. Kornecki, V. P. S. Awana, H. Kishan, S. Balamurugan, and E. Takayama-Muromachi, *J. Appl. Phys.* **101**, 09G104 (2007).

¹⁰A. Butera, A. Fainstein, E. Winkler, J. van Tol, S. B. Oseroff, and J. Tallon, *J. Appl. Phys.* **89**, 7666 (2001).

¹¹H. A. Blackstead, W. B. Yelon, P. J. McGinn, N. A. Licata, Q. Cai, D. Wang, and Z. Ren (unpublished).